Sensors and Actuators B 230 (2016) 206–211

Contents lists available at ScienceDirect

Sensors and Actuators B: Chemical

journal homepage: www.elsevier.com/locate/snb

Surface plasmon resonance refractive sensor based on silver-coated side-polished fiber

Jing Zhao, Shaoqing Cao, Changrui Liao, Ying Wang, Guanjun Wang, Xizhen Xu, Cailing Fu, Guiwen Xu, Jiarong Lian, Yiping Wang*

Key Laboratory of Optoelectronic Devices and Systems of Ministry of Education and Guangdong Province, Shenzhen University, Shenzhen 518060, China

ARTICLE INFO

Article history:
Received 30 November 2015
Received in revised form 30 January 2016
Accepted 5 February 2016
Available online 8 February 2016

Keywords:
Optical fiber sensor
Surface plasmon resonance
Side-polished fiber
Silver degradation

ABSTRACT

We demonstrate a surface plasmon resonance refractive sensor based on the side-polished single mode optical fiber and investigated the sensor performance decay induced by silver coating degradation. The sensor showed fast response to the refractive index liquid in the range from 1.32 to 1.40 RIU. The highest sensitivity up to 4365.5 nm/RIU and a FOM of 51.61 RIU^{-1} were achieved, which were comparable to the reported polished-fiber-based SPR sensors. Characteristics of the silver-coated sensor after exposure to the air as well as to the liquid environment were investigated. The sensor always stored in dry air could respond stably two weeks later with sensitivity comparable with the fresh one and lower resolution due to the broadened resonant dip. But the sensor immersed in the refractive liquid for 30 min firstly and then exposed to ambient air for hours decayed dramatically due to silver degradation. The presented silver-coated SPR sensor could be used as a simple, cost-effective, disposable device in bio-chemical, environment, and food safety detection.

1. Introduction

Surface Plasmon waves (SPW) are electron density oscillations where the associated Transverse Magnetic (TM) polarized electromagnetic waves are guided parallel to the metal-dielectric interface. Surface Plasmon resonance (SPR) can be excited at the interface between the thin metallic film and the dielectric media when the energy and momentum of the incident light match that of the SPW. The energy carried by photons was coupled to the electrons in a metal to achieve a sharp resonant dip in the light intensity. The propagation constant of the SPW strongly depends on the refractive index (RI) of the surrounding medium. Therefore, even very small changes in the RI adjacent to metal layer can produce a measurable shift in the resonant dip [1]. This property has been widely exploited in recent decades to develop SPR sensors used in disease diagnostics, food safety, environmental monitoring as well as in biological analysis and other sciences [2–5].

Traditionally, SPR is excited by an evanescent field produced by attenuated total reflection (ATR) in the prism configuration. With the tendency to miniaturization, the optical-fiber-based SPR allows for a smaller sample volume, real-time and label-free detection, and the sensor is based on the same principle as the prism coupling device. Since the time it was first proposed by Jorgenson and Yee more than two decades ago [6], many new types of SPR sensors based on optical fiber technology have been developed [7–11]. Specifically, a side-polished fiber (SPF) with the fiber cladding removed to access the evanescent field of the guide mode was designed to be coupled with the SPR technology due to, among others, low manufacturing cost, the flat polished surface good for depositing uniform metal film, and the strong evanescent field to excite SPR [12,13]. However, the cladding polishing or dissolution process decreased the fiber elasticity and mechanical strength, which sets a limitation for the reuse and life span of the SPF-based sensor. From a practical as well as commercial point of view, there still is a room for the simplification of the low-cost disposable SPF-based SPR sensor. Typically, the SPR sensors deposited with metals such as gold or silver have good RI response and high sensitivities. Silver-coated sensor enables sharpest resonant dip, higher resolution and lower cost than gold-coated sensor [14]. However, degradation of the silver in ambient air and moisture environment can change the metal composition and decrease the interfacial adhesion force of silver film [15–17], which limit the use of Ag-based SPR sensor in many applications. One of the goals of the study was to evaluate how silver degradation influences the sensing performance of SPR devices. Here, we demonstrate a simple silver-coated SPR sensing scheme based on the side polished sin-

* Corresponding author.
E-mail address: ypwang@szu.edu.cn (Y. Wang).

http://dx.doi.org/10.1016/j.snb.2016.02.020
0925-4005/

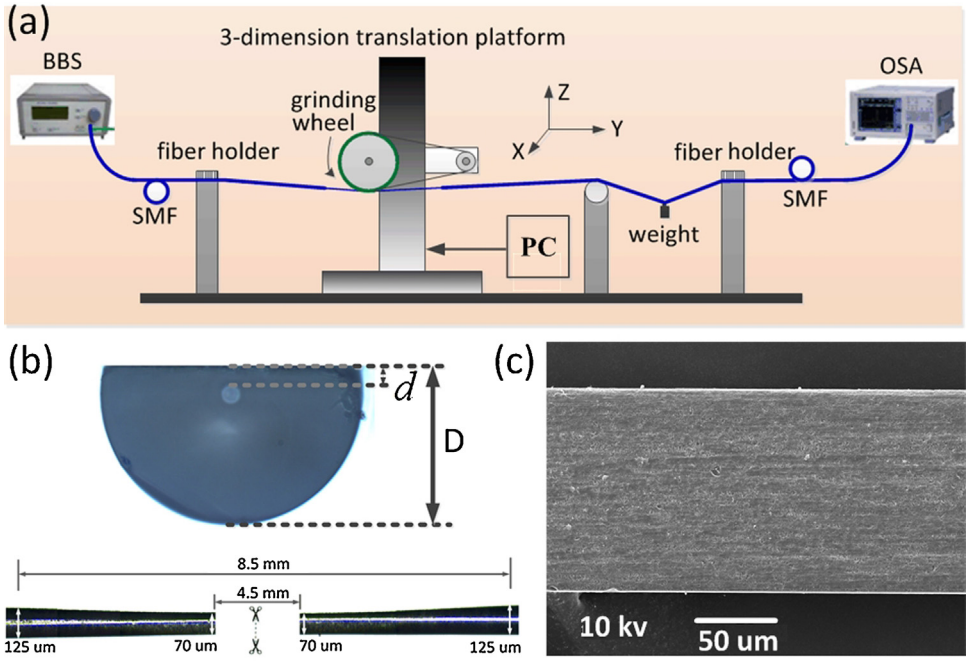

Fig. 1. (a) Schematic diagram of the wheel polishing setup to fabricate SPF; (b) The cross and longitude section of the D-shape SPF observed by microscope; and (c) overview of the polished surface of SPF observed by 500X SEM.

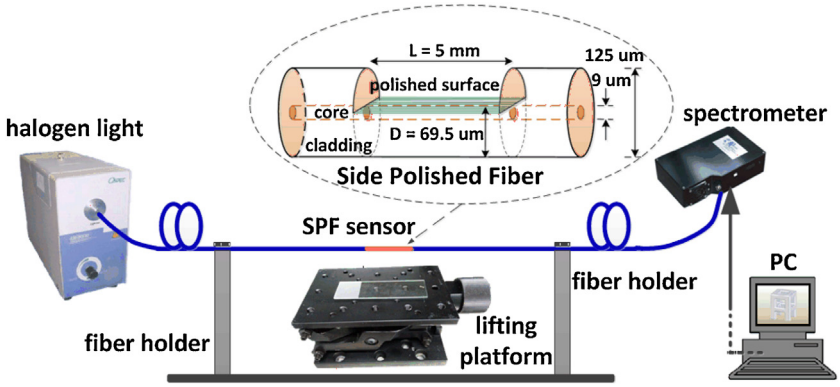

Fig. 2. Schematic diagram used to test the RI response of the SPR sensor, insertion is the structure diagram of the SPF-based SPR sensor.

gle mode fiber, and characterize the performance decay induced by silver degradation after it was exposed to the dry air or the liquid environment.

2. Methods of device fabrication

Side-polished fiber used in the experiment was fabricated by the wheel polishing technique developed by our group [18]. Fig. 1a shows the schematic of the wheel polishing setup (WanRun Ltd., WuXi, China) which was used in the study. A cylinder grinding wheel was fastened on a precise 3-dimension translation platform that can move along the X, Y and Z directions via computer control. A standard single mode optical fiber (Corning SMF-28) with a core/cladding diameter of 8.2/125 μm was fixed by a pair of fiber holders. A small section of fiber coating was stripped off in advance. The abrasive paper fasted around the mechanical wheel was found to be a key factor influencing the smoothness of polished surface. Here, we chose different roughness of 5000, 7000, and 10000-mesh abrasive papers (Warriors 991A, STABCKE, Germany) with grain size of 2.6 μm, 1.8 μm, and 1.3 μm to fast polish fiber in sequence. The cross section and longitude side view of the D-shape SPF were observed by a microscope as shown in Fig. 1b, where '*D*' and '*d*' represent the thickness of the residual fiber and cladding, respectively. It can be found that among the two 2 mm-tapered transition regions was the flat effective acting region, which is the actual sensing area of SPF. The polished surface of SPF was observed by the 500X Scanning Electron Microscope (SEM) as shown in Fig. 1c. During the polishing process, the transmission spectrum of SPF was monitored in-line by an optical spectrum analyzer (OSA, YOKOGAWA AQ6370C) and a broadband light source (BBS) in the range from 1250 to 1650 nm. Eventually, the polishing process was stopped at the stage when SPF was polished near to the fiber core region and with the power loss of approximately 1 dB in air.

Thin silver film was further coated on the flat surface of SPF by vacuum thermal evaporation system (Shenyang ZKY Co., Ltd.) to excite SPR. SPF samples were fixed on a metallic turntable with the polished surface faced upwards. To obtain a uniform coating, the turntable rotated horizontally at a constant speed in the vacuum cavity evacuated to 5×10^{-5} Pa. The thickness of silver film was monitored by a quartz-crystal detector during the deposition process. Parameters of the SPR sensor including the thickness of silver film (h), residual fiber thickness (D) and the length of sensing

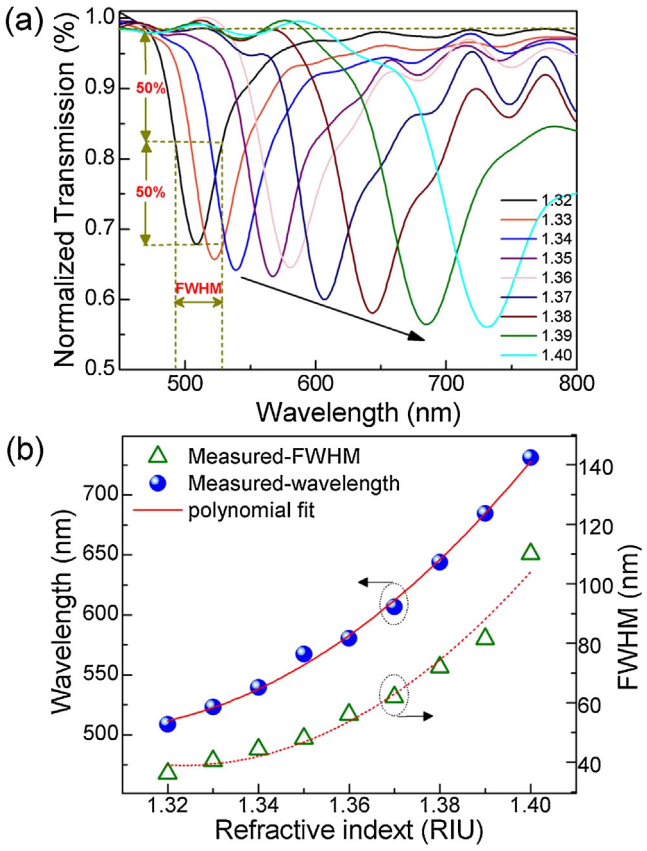

Fig. 3. (a) Normalized transmission spectra of SPR-1 test immediately in the index-matching liquid from 1.32 to 1.40 RIU; and (b) the non-linear relation between the wavelength shift and FWHM versus RI variation.

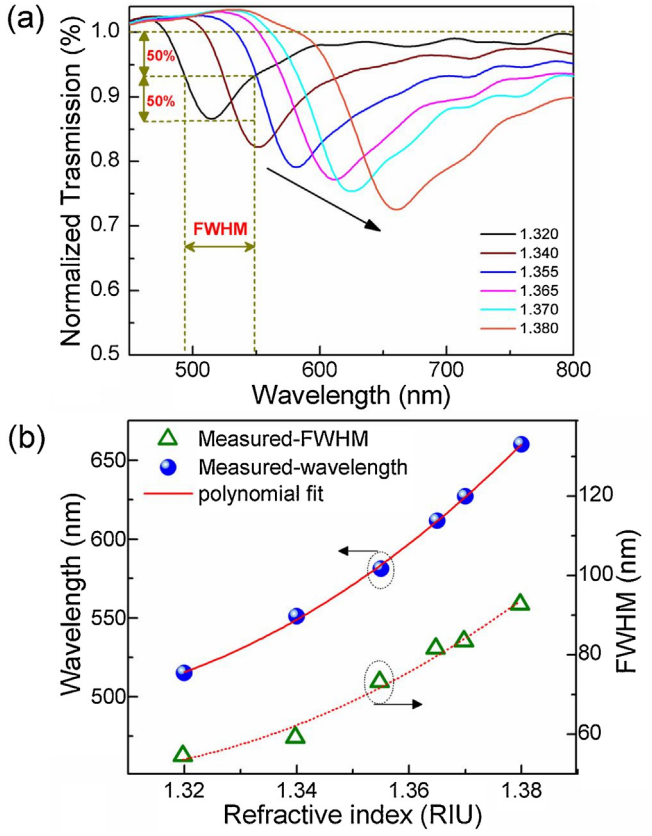

Fig. 4. (a) Normalized transmission spectra of SPR-2 stored in air for two weeks, tested in the index-matching liquid from 1.32 to 1.38 RIU; (b) the non-linear relation between the wavelength shift and FWHM versus RI variation.

region (L) was optimized according to the literature[19,20]. Here, we fabricated SPR sensors by use of SPFs with power loss around 1 dB, $D = 69.0 \pm 0.8$ μm, $L = 5$ mm, and coating with silver film with $h = 40$ nm to practically maximize the SPR performance.

3. Evaluation of refractive index response

Wavelength interrogation method was used to characterize the proposed SPR sensor. Experimental setup is presented in Fig. 2 and includes a Tungsten halogen light source (100W, LS-3000, Ocean Optics), a SPF-based sensor, and a spectrometer (USB65000, Ocean Optics) with detection range from 200 to 1100 nm. As a substitution for the typical pump-driven micro-fluidic cell, a simple testing platform composed of a manual lifting platform, fiber holders, and glass slide was proposed to test the SPR sensor's response. The inset of Fig. 2 illustrates the structure of SPF-based SPR sensor. During the test process, the SPR sensor was naturally straightened and fixed on both sides by fiber holders. All the light joint parts were fixed to reduce the fiber deformation and fluctuations in the polarization of transmitted light. The distribution of the incident wave angles was assumed to be constant. When a drop of the index matching liquid is on the glass slide, the height of lifting platform needs to be adjusted manually and then the active sensing region of the sensor can be immersed in the refractive liquid. Finally, the transmission outputs of the SPR sensor in the refractive liquid as well as in the air were recorded respectively at room temperature by the spectrometer, all above the noise of the background. It is important to rinse the SPR sensor with alcohol repeatedly between each subsequent measurement to ensure that the polished surface is clean.

4. Result and discussion

To investigate the influence of silver coating degradation on the performance of the sensor, the silver-coated SPR sensors with the same parameters were divided into two groups: SPR-1 which was tested immediately and SPR-2 which was exposed to an oxygen-containing dry air for two weeks. Fig. 3a shows the experiment transmission spectra of SPR-1 tested immediately in different index-matching liquids (Cargille Labs, http://www.cargille.com) where refractive index unit (RIU) varied from 1.32 to 1.40. The normalized spectrum was obtained from the percentage of the transmitted photon counts when the sensor was immersed in liquid compared to the transmittance of the sensor exposed to air. A series of regular resonant dips exist in the normalized transmission spectrum which results from coupling the energy from the fiber guide mode to SPW in proximity to silver film at the resonant wavelength. With the increase of refractive index, a red shift of the central dip position changed from 508 to 731 nm. Here, some unwanted fluctuations in the output spectra in Fig. 3a were induced by the little fiber deformations generated during the test process when SPF was repeatedly immersed in the RI liquid and washed by alcohol with the up-and-down lifting platform. This little fiber deformation could cause the polarization fluctuations of the light interacting with the SPW and then produce the noise wave beside the SPR dips. To obtain more stable SPR spectra, polarization-maintaining or depolarization method can be used in experiment [19,20].

The sensitivity of the SPR sensor based on spectral interrogation was defined as $S = \Delta\lambda/\Delta n$, where Δn was the variable value of refractive index and $\Delta\lambda$ was the corresponding central wavelength shift of the resonant dips. Fig. 3b illustrates the non-linear relation between the wavelength shifts versus RI variation. The slopes of

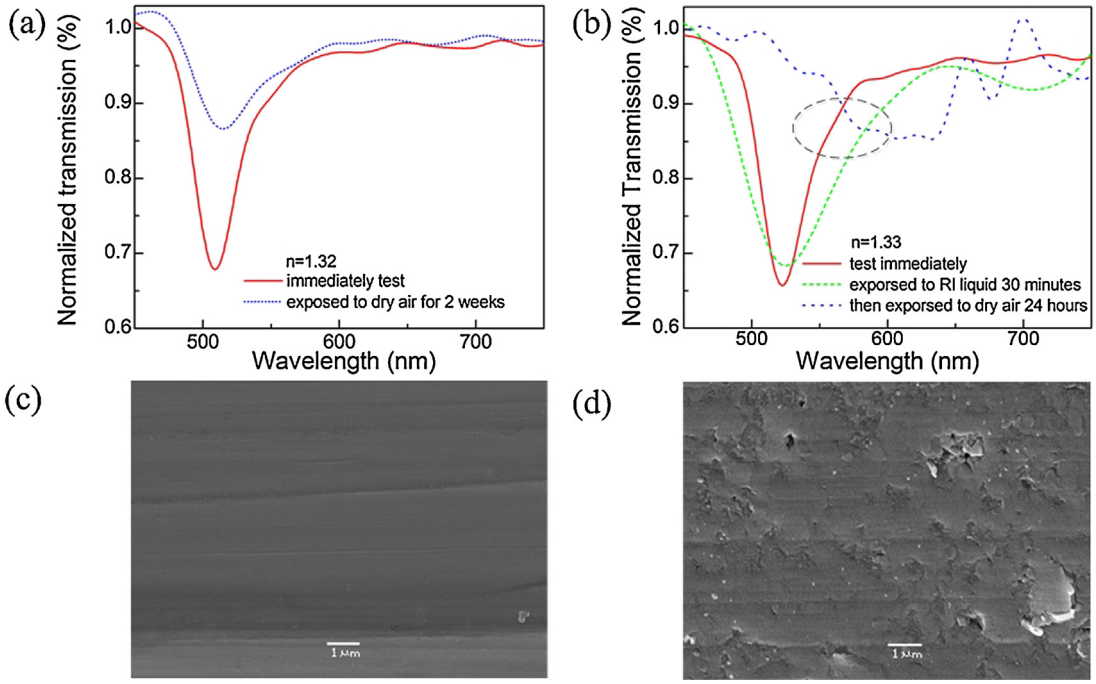

Fig. 5. (a) Resonant dips of the SPR sensor tested immediately versus the one stored in dry air for two weeks, and (b) evolution of SPR dip tested immediately, after immersing in liquid for 30 min, exposed to ambient air for 24 h; SEM image of the silver surface for (c) the sensor stored in dry air for two weeks, and (d) the sensor exposed in liquid 30 min and then stored in ambient for two weeks.

Table 1
Characteristics of the SPR-1 tested immediately in index-matching liquid from 1.320 to 1.400 RIU.

Range (RIU)	Δλ (nm)	Sensitivity (nm/RIU)	Av.FWHM (nm)	$б_{sp}$ (nm)	Resolution (RIU)	Av.FOM (RIU^{-1})
1.320–1.340	30.47	1523.5	39.3	3.7	2.42×10^{-3}	38.76
1.340–1.360	41.24	2062.0	46.7	4.4	2.13×10^{-3}	44.15
1.360–1.380	63.38	3169.0	61.4	5.8	1.83×10^{-3}	51.61
1.380–1.400	87.31	4365.5	87.7	8.3	1.90×10^{-3}	49.77

the curve was the value of sensitivity. To calculate the sensitivity in a relative linear region, the detection RI from 1.32 to 1.40 was divided into four ranges. The sensitivities provided along with other parameters are shown in Table 1. With the increase of RI, sensitivity of the proposed SPR sensor raised from 1523.5 to 4365.5 nm/RIU. The maximal sensitivity achieved surpassed that of the SPF-based SPR sensor reported by R. Slavik (3150 nm/RIU) [19] and close to that of the SPR fiber sensor fabricated by the controllable hybrid polishing method (5100 nm/RIU) [13].

The resolution of the SPR sensor, R, was defined as $R = \sigma/S$, where σ represents the smallest measurable wavelength and S was the sensitivity measured in experiment [21]. σ can be measured as the standard deviation of the resonant wavelength by statistical experiments [22] or estimated by the equation as [23]:

$$\sigma = \frac{\mathrm{FWHM}}{4.5 \times \sqrt[4]{\mathrm{SNR}}} \quad (1)$$

Here, SNR of the spectrometer (USB65000, Ocean Optics) we used was 30 dB. FWHM was the full width at half minimum of the typical resonances spectrum, and defined as the corresponded wavelength width at the half percentage of the normalized resonant dip. For example, FWHM of the resonant dip in refractive liquid ($n = 1.32$) is illustrated in Fig. 3a. The non-linear relation between FWHM versus RI variation is shown in the right side of Fig. 3b. With the increase of RI, the average FWHM in the four RI range increased from 39.3 to 87.7 nm (Table 1). Thus, the calculated σ changed from 3.7 to 8.3 nm according to Eq. (1). With the sensitivity values obtained in Table 1, the average resolutions in the four RI ranges are estimated to vary from 2.42×10^{-3} to 1.83×10^{-3} RIU. To comprehensively characterize the performance of SPR sensor, the figure of merit (FOM) was defined as FOM = S/FWHM. Here, average FOMs in the four RI ranges changed from 38.76 to 51.61 RIU^{-1}. These values compare favorably with the reported FOM for the gold-nanoparticles-array LSPR sensor (maximum of 40 RIU^{-1}) [24] and the theoretical value of the comb-like silver nano strips (maximum of 40–343.6 RIU^{-1}) [25]. The maximal FOM as well as the lowest resolution was obtained in the detection range from 1.38 to 1.40 RIU, which seems to be the optimal working range for the presented sensor.

The SPR-2 experiment was conducted in the same way but with exposure to the dry air for two weeks. As shown in Fig. 4a, the increase of RI from 1.32 to 1.38 resulting in the resonance wavelength shifted from 515 to 660 nm. The non-linear relationship of the resonant wavelength shift as well as FWHM versus refractive index is shown in Fig. 4b. This relationship seems similar to that shown in Fig. 3b for the SPR-1. Table 2 summarizes the characteristic parameters of the SPR-2 experiment. Sensitivity increased from 1798.0 to 3237.3 nm/RIU in the RI range from 1.32 to 1.38 RIU, which is comparable with that of 1523.5–3169.0 nm/RIU for SPR-1 without storage. However, the resonant dips of SPR-2 became shallower and wider obviously. FWHM varied from 58.6 to 81.0 nm, which was larger than that from 39.3 to 61.4 nm for SPR-1 in the same detection range. Accordingly, the resolution of SPR-2 decreased, and the highest value of FOM was reduced to 39.97 RIU^{-1}. These results suggest that the sensitivity of silver-coated SPR sensor was not significantly affected by exposure in air for two

Table 2
Characteristics of the SPR-2 exposed in dry air for two weeks, tested in the index-matching liquid from 1.320 to 1.380 RIU.

Range (RIU)	Δλ (nm)	Sensitivity (nm/RIU)	Av.FWHM (nm)	σ_{sp} (nm)	Resolution (RIU)	Av.FOM (RIU^{-1})
1.320–1.340	35.96	1798.0	58.6	5.4	3.00×10^{-3}	30.68
1.340–1.365	60.53	2421.2	72.6	6.7	2.76×10^{-3}	33.35
1.365–1.380	48.56	3237.3	81.0	7.5	2.31×10^{-3}	39.97

weeks. However, the sensor's resolution as well as FOM decreased a little due to the silver degradation in air. Generally, the performance of SPR-2 stored in the dry air for two weeks was still comparable to the reported SPF-based SPR sensors [26–28].

Further analysis examined the influence of the surrounding environment on the parameters of the silver-coated sensor exposed to air as well as liquid. Fig. 5a compares the normalized transmission spectra of the sensor stored in the dry atmosphere (sealed container with desiccant) for two weeks and the one tested immediately in the refractive liquid with $n = 1.32$. It appears that the resonant dip of the air-exposed sensor decayed a little when compared to the one with fresh silver coating, and the central position of resonance did not change. Fig. 5c shows the SEM image of silver surface for the air-exposed sensor. The surface is smooth without obvious deterioration, and the tiny stripes were the surface scratches on SPF generated during the polishing process by abrasive. This well-preserved surface is supported by the fact that the silver coating does not ordinarily deteriorate for a long time as long as the coating is perfectly sealed in a dry atmosphere [16], which explained the little performance degradation in SPR-2.

However, the sensor exposed to liquid environment was affected in a different way. Here, the sensor was immersed in the refractive liquid for 30 min to imitate the actual exposure process during the RI testing. Subsequently it was washed by alcohol repeatedly to remove the residue on sensing area, and then stored naturally in the super-clean atmosphere (e.g. 24 h, 20 °C, 45% relative humidity). Fig. 5b illustrates the resonance evolution of the sensor with fresh silver coating, after immersing in liquid for 30 min, and then exposed to ambient air for 24 h. These resonant dips were all tested in the water environment ($n = 1.33$). As is apparent from the figure, the exposure to RI liquid for 30 min itself contribute a little resonance degradation, including a small central position shift and a broader resonance width. However, after the exposed-to-liquid sensor stored in ambient air for hours, the transmission fringe deformed significantly. These phenomena can be explained as the exposure to refractive liquid decreased the surface crystal state and triggered the moisture-induced deterioration of silver layer [16]. The SPR dip position as well as its FWHM depends strongly on the oxidation level of silver [17]. Thus, short contacting with liquid induced a little performance decay by silver degradation in the first 30 min. In the following process of exposure to ambient air, moisture was considered to penetrate into the silver layer and enhance the migration of the silver ion. Then destructive degradation of the sensing performance occurs. To reinforce the effect of this moisture induced deterioration, the exposed-to-liquid sensor was stored in ambient for another two weeks. Fig. 5d illustrates the deteriorated silver surface with shallow dimples and peeling silver layer. The exposing to liquid accelerated silver's degradation. Thus, unlike SPR-2 only exposed in dry air, degradation of the silver-based sensor exposed in liquid seems destructive for the performance of the sensor. So the presented silver-coated SPR sensor would no longer be used after one-round of test.

5. Conclusion

The silver-coated SPR refractive sensor based on the side-polished fiber was fast fabricated by our wheel polishing technique and we characterized its performance as a function of silver coating degradation. The proposed SPR sensor exhibited fast response to the refractive liquid ranging from 1.32 to 1.40 RIU. With the increase of RI, both sensitivity and FWHM increased significantly and followed a non-linear relationship. Sensitivity up to 4365.5 nm/RIU and a highest FOM of 51.61 RIU^{-1} were obtained in the optimal detection range from 1.38 to 1.40 RIU. Performance decays of the studied sensors were evaluated in exposure to the dry ambient air as well as to the refractive liquid. The comparison showed that the sensor stored in air could respond more stably two weeks later with sensitivity comparable with that of the fresh one, but with somewhat lower resolution due to the broadened resonant dip. As the exposure to liquid triggered the moisture-induced deterioration of silver which was destructive for the sensor, it is recommended for storage only in dry inert atmospheres and should not be reused after one-round of test. The proposed silver-coated SPR sensor could be used as a cost-effective, real-time disposable device with numerous applications in bio-chemical, environment, food safety detection, and other industrial and academic settings.

Acknowledgements

This work was supported by National Natural Science Foundation of China (grant nos. 61425007, 61377090, 61575128, and 61405127), Guangdong Provincial Department of Science and Technology (grants nos. 2014A030308007, 2014B050504010, and 2015B010105007), Science and Technology Innovation Commission of Shenzhen/Nanshan (grants nos. ZDSYS20140430164957664, KC2014ZDZJ0008A, GJHZ20150313093755757), and Pearl River Scholar Fellowships.

References

[1] H. Jirí, Surface plasmon resonance sensors for detection of chemical and biological species, Chem. Rev. 108 (2008) 462–493.
[2] K. Bremer, B. Roth, Fibre optic surface plasmon resonance sensor system designed for smartphones, Opt. Express 23 (2015) 17179–17184.
[3] J. Pollet, F. Delport, K.P.F. Janssen, D.T. Tran, J. Wouters, T. Verbiest, et al., Fast and accurate peanut allergen detection with nanobead enhanced optical fiber SPR biosensor, Talanta 83 (2011) 1436–1441.
[4] S. Herranz, M. Bockova, M.D. Marazuela, J. Homola, M.C. Moreno-Bondi, An SPR biosensor for the detection of microcystins in drinking water, Anal. Bioanal.Chem. 398 (2010) 2625–2634.
[5] J. Pollet, F. Delport, K.P.F. Janssen, K. Jans, G. Maes, H. Pfeiffer, et al., Fiber optic SPR biosensing of DNA hybridization and DNA-protein interactions, Biosens. Bioelectron. 25 (2009) 864–869.
[6] R.C. Jorgenson, S.S. Yee, A fiber optic chemical sensor based on surface plasmon resonnace, Sens. Actuators B: Chem. 12 (1993) 213–220.
[7] H. Esmaeilzadeh, M. Rivard, E. Arzi, F. Legare, A. Hassani, Smart textile plasmonic fiber dew sensors, Opt. Express 23 (2015) 14981–14992.
[8] M.-C. Navarrete, N. Díaz-Herrera, A. González-Cano, Ó. Esteban, Surface plasmon resonance in the visible region in sensors based on tapered optical fibers, Sens. Actuators B: Chem. 190 (2014) 881–885.
[9] Y. Zhao, Z.-q. Deng, J. Li, Photonic crystal fiber based surface plasmon resonance chemical sensors, Sens. Actuators B: Chem. 202 (2014) 557–567.
[10] M.D. Baiad, R. Kashyap, Concatenation of surface plasmon resonance sensors in a single optical fiber using tilted fiber Bragg gratings, Opt. lett. 40 (2015) 115–118.
[11] R. Garg, S.M. Tripathi, K. Thyagarajan, W.J. Bock, Long period fiber grating based temperature compensated high performance sensor for bio-chemical sensing applications, Sens. Actuators B: Chem. 176 (2013) 1121–1127.
[12] H.-Y. Lin, W.-H. Tsai, Y.-C. Tsao, B.-C. Sheu, Side-polished multimode fiber biosensor based on surface plasmon resonance with halogen light, Appl. Opt. 46 (2007) 800–806.
[13] H. Esmaeilzadeh, E. Arzi, F. Légaré, M. Rivard, A. Hassani, A super continuum characterized high precision SPR fiber optic sensor for refractometry, Sens. Actuators A: Phys. 229 (2015) 8–14.

[14] M. Mitsushio, K. Miyashita, M. Higo, Sensor properties and surface characterization of the metal-deposited SPR optical fiber sensors with Au, Ag, Cu, and Al, Sens. Actuators A: Phys. 125 (2006) 296–303.
[15] H. Sahm, C. Charton, R. Thielsch, Oxidation behaviour of thin silver films deposited on plastic web characterized by spectroscopic ellipsometry (SE), Thin Solid Films 455 (2004) 819–823.
[16] E. Ando, M. Miyazaki, Moisture degradation mechanism of silver-based low-emissivity coatings, Thin Solid Films 351 (1999) 308–312.
[17] J.M.J. Santillan, L.B. Scaffardi, D.C. Schinca, F.A. Videla, Determination of nanometric Ag_2O film thickness by surface plasmon resonance and optical waveguide mode coupling techniques, J. Opt. 12 (2010).
[18] J. Zhao, G.L. Yin, C.R. Liao, S. Liu, J. He, B. Sun, et al., Rough side-polished fiber with surface scratches for sensing applications, IEEE Photonics J. 7 (2015).
[19] R. Slavik, J. Homola, E. Brynda, A miniature fiber optic surface plasmon resonance sensor for fast detection of staphylococcal enterotoxin B, Biosens. Bioelectron. 17 (2002) 591–595.
[20] M. Piliarik, J. Homola, Z. Maníková, J. Čtyroký, Surface plasmon resonance sensor based on a single-mode polarization-maintaining optical fiber, Sens. Actuators B: Chem. 90 (2003) 236–242.
[21] M. Piliarik, J. Homola, Surface plasmon resonance (SPR) sensors: approaching their limits? Opt. Express 17 (2009) 16505–16517.
[22] B.-H. Liu, Y.-X. Jiang, X.-S. Zhu, X.-L. Tang, Y.-W. Shi, Hollow fiber surface plasmon resonance sensor for the detection of liquid with high refractive index, Opt. Express 21 (2013) 32349–32357.
[23] I.M. White, X. Fan, On the performance quantification of resonant refractive index sensors, Opt. Express 16 (2008) 1020–1028.
[24] P. Offermans, M.C. Schaafsma, S.R.K. Rodriguez, Y. Zhang, M. Crego-Calama, S.H. Brongersma, et al., Universal scaling of the figure of merit of plasmonic sensors, ACS Nano 5 (2011) 5151–5157.
[25] O.V. Shapoval, Comparison of refractive-index sensitivities of optical-mode resonances on a finite comb-like grating of silver nanostrips, IEEE J. Quantum Electron. 51 (2015).
[26] J. McPhillips, A. Murphy, M.P. Jonsson, W.R. Hendren, R. Atkinson, F. Höök, et al., High-performance biosensing using arrays of plasmonic nanotubes, ACS Nano 4 (2010) 2210–2216.
[27] E.A. Velichko, A.I. Nosich, Refractive-index sensitivities of hybrid surface-plasmon resonances for a core–shell circular silver nanotube sensor, Opt. Lett. 38 (2013) 4978–4981.
[28] C. Caucheteur, T. Guo, J. Albert, Review of plasmonic fiber optic biochemical sensors: improving the limit of detection, Anal. Bioanal. Chem. 407 (2015) 3883–3897.

Biographies

Jing Zhao is a Ph.D student in optical engineering of Shenzhen University. She received bachelor degree in Applied Chemistry from Chengdu University of Technology, and master degree in Microelectronics from University of Electronic Science and Technology of China. She has worked as an Integrated Circuit thin film engineer in the CTEC-24 institute, and as a high speed PCB designer in Huawei Technologies CO., LTD before her Ph.D research. Her current research interests are SPR optical fiber sensor and bio-chemical sensors.

Shaoqing Cao was born in Hunan province in China in 1992. He is currently completing his master degree in the field of fiber optic sensors at Shenzhen University, China.

Changrui Liao received B.Sc. and M.Eng. degree from School of Optical and Electronic Information, Huazhong University of Science and Technology, China in 2005 and 2007. He received Ph. D. degree from Department of Electrical Engineering, The Hong Kong Polytechnic University in 2012. Since 2012, he has been with College of Optoelectronic Engineering, Shenzhen University as a lecturer. His research interest is focused on optical fiber sensors and femtosecond laser micromachining. He has authored or coauthored 8 patents and more than 70 journal and conference papers.

Ying Wang received his B.Sc. degree in Applied Physics, and Ph.D. degree in Physical Electronics from Huazhong University of Science and Technology (Wuhan, China) in 2004 and 2010, respectively. He worked in Department of Electrical Engineering, The Hong Kong Polytechnic University (Hong Kong, China) as a research associate from 2010 to 2015, and joined in College of Optoelectronic Engineering,Shenzhen University as a lecturer in 2015. His research interests are optical fiber sensors and femtosecond laser micromachining.

Guanjun Wang received the Ph.D. degree from Beijing University of aeronautics and astronautics. He is currently a post-doctor in Shenzhen University, and focus on Bio-chemical optical fiber sensor.

Xizhen Xu was born in Guangdong province, China, in 1990. He is currently completing his master degree in the field of fiber optic sensors at Shenzhen University, China

Cailing Fu received her M.S. degree from the science department of Wuhan Institute of Technology, China, in 2015. She is currently a Ph.D. student at Shenzhen University, focus on the fiber optic sensors.

Guiwen Xu is the assistant researcher in the College of Optoelectronic Engineering, Shenzhen University, responsible for the management of the public analysis and test experimental platform.

Jiarong Lian is the associate professor in the College of Optoelectronic Engineering, Shenzhen University. He received the Ph.D. degree in condensed matter physics from Sun Yat-Sen University in 2008. His research interests are thin film materials and devices, OLED.

Yiping Wang was born in Chongqing, China, in 1971. He is a Professor and Pearl River Scholar in the College of Optoelectronic Engineering, Shenzhen University. He received the B.S. degree in Precision Instrument Engineering from Xi'an Institute of Technology in 1995, and the M.S. degree in Precision Instrument and Mechanism and the Ph.D. degree in Optical Engineering from Chongqing University in 2000 and 2003. He worked as a postdoctoral research fellow in the Department of Electronics Engineering of Shanghai Jiao Tong University in 2003, and in the Department of Electrical Engineering of Hong Kong Polytechnic University in 2005. He joined the Institute of Photonic Technology, Jena, Germany as a Humboldt research fellow in 2007, and joined the Optoelectronics Research Centre, University of Southampton, U.K. as a Marie Curie Fellow in 2009. His current research interests focus on optical fiber sensors, in-fiber gratings, photonic crystal fibers, and Biochemical fiber sensors. He has authored or coauthored 1 book, 9 patent applications, and more than 150 journal and conference papers with a SCI citation of more than 1200 times. Dr. Wang is a senior member of IEEE, the Optical Society of America, and the Chinese Optical Society.